MJFAS
Malaysian Journal of Fundamental and Applied Sciences

Tan *et al.* | Malaysian Journal of Fundamental and Applied Sciences, Vol. 21 (2025) 2045-2056

RESEARCH ARTICLE

A Comparative Analysis of Different Color Spaces for Paddy Maturity Assessment Using Drone Imagery

Ji Loun Tan[a], Mastang Tanra[b], Muhammad Mukhlisin[c], Amin Suharjono[d], Irfan Mujahidin[d], Catur Budi Waluyo[d], Rizkha Ajeng Rochmatika[d], Fatardho Zudhi[e], Norhana Arsad[a]*

[a]Department of Electrical, Electronic and Systems Engineering, Faculty of Engineering and Built Environment, Universiti Kebangsaan Malaysia, Bangi 43600, Selangor, Malaysia; [b]Universitas Muhammadiyah Cileungsi, Jl. Anggrek No.25, Perum. PTSC, Cileungsi, Kec. Cileungsi, Kabupaten Bogor, Jawa Barat 16820, Indonesia; [c]Department of Civil Engineering, Politeknik Negeri Semarang, Jl. Prof. Soedarto SH, Tembalang, Semarang, Jawa Tengah 50275, Indonesia; [d]Department of Electrical Engineering, Politeknik Negeri Semarang, Jl. Prof. Soedarto SH, Tembalang, Semarang, Jawa Tengah 50275, Indonesia; [e]Politeknik Pertanian Negeri Payakumbuh, Jl. Raya Negara Km. 7 Tajung Pati, Kecamatan Harau, Kabupaten Limapuluh Kota, Sumatera Barat 26271, Indonesia

Abstract Paddy is a staple food for a large portion of the global population with Asia accounting for about 90% of the world's rice production. The accurate detection of paddy maturity is important to optimizing harvest time, ensuring maximum yield and reducing post-harvest losses. Traditional methods of assessing paddy ripeness are labour-intensive and prone to human error, hence required the development of efficient and automation approaches. This study explores the effectiveness of drone imagery and image processing to assess paddy maturity at two ripeness stages which are unripe and ripe (ready for immediate harvest). High-resolution images of paddy fields in a district of an ASEAN country were captured and processed using MATLAB software to analyze four color spaces include RGB, HSV, YCbCr and L*a*b*. The results show that the RGB and HSV color spaces reflect shifts in red/green intensities and hues during ripening. YCbCr shows the changes in chrominance components between the unripe and ripe stages. However, the L*a*b* color space proved to be the most effective, offering the highest distinction between ripe and unripe paddy in L*, a*, and b* values, which closely align with the expected visual ripeness characteristics. This study has suggested that integrating this method with machine learning could enable real-time, automated crop monitoring, improving harvest timing and overall crop management.

Keywords: Color space, drone imagery, image processing, machine learning, paddy maturity.

***For correspondence:**
noa@ukm.edu.my

Received: 19 Sept. 2024
Accepted: 29 April 2025

Introduction

Paddy, which is known as rice is a staple food for a significant portion of the global population with Asia accounting for about 90% of the world's rice production [1, 2]. Malaysia is an agricultural country with large farming lands, which views political stability and food security as being strongly connected to its extensively regulated and subsidized rice industry [3]. Similarly, for in Indonesia, the agricultural sector especially rice production is very important, as rice is the main staple diet for most of the population in the country [4]. In 2016, Malaysians consumed 2.7 million tons of rice, with approximately 67% produced domestically and the rest of rice imported from nearby countries which including Thailand, India, Vietnam, and Pakistan [3]. In addition, Malaysian adults consume an average of 2.5 plates of white rice

per day, highlighting rice as the most important crop in the food subsector, hence due to the important link between food security and rice security, the Malaysian government has made rice production self-sufficiency a national policy [5, 6].

Due to the importance of rice, accurate detection of paddy maturity is very important for optimal harvesting, ensuring maximum yield and minimizing post-harvest losses. Traditional methods of assessing paddy maturity, which often rely on manual inspection, can be labor-intensive, time-consuming, and prone to human error. As the population grows, the demand for rice is expected to rise significantly, potentially exceeding domestic production capabilities [7]. In addition, climate change may profoundly impact rice yields across Asia and the Pacific, threatening food security in many countries and exacerbating challenges for rice producers [4, 8]. Studies have shown that climate change significantly affects Malaysian paddy yields, prompting efforts to prevent potential food shortages [9, 10, 11].

Recent advances in remote sensing and precision agriculture have highlighted the potential of drone technology in agricultural monitoring [12]. Drones equipped with multispectral and hyperspectral cameras can capture detailed imagery of large fields, providing data that can be analyzed to gain insights into crop health and development [13]. This approach by combining high spatial resolution images with accurate segmentation algorithms can allows for the identification of key indicators of crop maturity that are not easily discernible through conventional methods [14].

Non-destructive determination of crop maturity is important for obtaining save time and cost effective information about optimal harvest time and crop management, hence image processing techniques offer one of the solution for predicting crop maturity, which allowing for accurate assessment without damaging the crops [15, 16]. By analyzing digital images, this image processing method enables the detection of changes in crop appearance that signal ripeness such as color of paddy. Additionally, image processing can be used to identify specific features, such as spots in paddy images, through the application of segmentation techniques, further enhancing its applications in agricultural management [17].

The primary objective of this research is to evaluate the effectiveness of various color spaces in distinguishing between two different stages of paddy maturity which are unripe and ripe (ready for harvest on the same day). Additionally, this study will evaluate the performance of various color space methods, including Red-Green-Blue (RGB), Hue-Saturation-Value (HSV), YCbCr (Luminance (Y), Chroma Blue (Cb), Chroma Red (Cr)), and Lab* (Luminance (L*), Green-Red Component (a*), Blue-Yellow Component (b*)). The objective is to identify the most suitable method for assessing and classifying paddy maturity levels through image analysis.

Methodology

The methodology of this study is divided into three main parts which are data collection, image processing and color space analysis. Data were collected using a drone equipped with a high-resolution camera to capture imagery of paddy fields. The captured images were processed and analyzed using MATLAB software. Each image was converted into four different color spaces analysis which are RGB, HSV, YCbCr and L*a*b* to facilitate a comprehensive comparison of color properties for ripeness detection. The workflow for the study of color spaces for paddy maturity detection using drone imagery is shown at Figure 1.

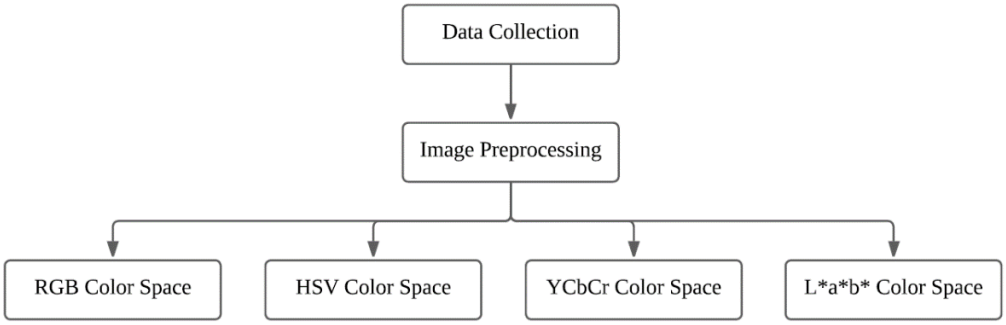

Figure 1. Workflow for the study of color spaces for paddy maturity detection using drone imagery

Data Collection

The data for this research were collected using a drone equipped with a high-resolution camera to capture imagery of paddy fields located in a district of an ASEAN country as shown in Figure 2. The selected paddy fields were categorized into two distinct maturity stages which are unripe and ripe, each representing different phases of crop readiness for harvest.

Figure 2. Location of data collection

In the unripe stage, the paddy was nearing maturity, with the expected harvesting process estimated to occur within one week. For the ripe stage, the paddy was ready for immediate harvesting and marked by prominent visual indicators of full ripeness such as the yellowing of the crops.

The drone imagery was collected at an altitude of approximately 20 meters to ensure a balance between field coverage and image resolution. The images were captured during optimal daylight hours to minimize lighting variations, which could impact the color information that important for ripeness detection. The drone followed along predefined flight paths to ensuring full coverage of the paddy field while maintaining consistent overlap between adjacent images for seamless processing. The images were georeferenced to ensure accurate spatial alignment for subsequent analysis.

Image Preprocessing

After the images were captured, the images underwent a series of preprocessing steps to ensure consistency and enhance the accuracy of the analysis, the steps were included image calibration, cropping and alignment and resolution adjustments.

Calibration was performed to correct and prevent for any distortions caused by the camera lens or environmental conditions. This step also ensured that all images maintained consistent color balance and brightness levels, minimizing the effects of shadows or cloud cover that could interfere with color space analysis.

The raw images were cropped to focus on specific areas of interest which are those sections of the field that contained the target paddy plants in different ripeness stages. Misaligned or blurred images were discarded to maintain data quality hence this process ensured that the analysis focused solely on relevant parts of the field, avoiding potential noise from non-paddy objects.

In addition, the images were resized to a 300 x 300 pixels consistent resolution for uniform analysis across different color space techniques. This ensured that pixel-level comparisons between color spaces would be fair and more standardized. The image of before and after preprocessing is shown in Figure 3.

Figure 3. Image of before and after preprocessing

Image Analysis

The processed images were analyzed using MATLAB software, each image was converted into four different color spaces which are RGB, HSV, YCbCr, and L*a*b* as shown in Figure 4 to facilitate a comprehensive comparison of color properties for ripeness detection. The selection of these color spaces is grounded in their ability to represent color information in different forms, potentially revealing different aspects of paddy ripeness.

Figure 4. RGB, HSV, YCbCr, and L*a*b* color spaces in MATLAB software

For RGB color space which commonly used in digital imaging, where represents each pixel through three intensity values corresponding to red, green, and blue components [18, 19]. In this study, the images were analyzed to monitor the transition from green to yellow during the paddy's ripening process.

In addition, the HSV color space separates color info into three components which are hue, saturation, and value of brightness [20, 21, 22]. This distinction between color and brightness is benefits for analyzing the subtle shifts from green to yellow as the paddy ripens. This study required particular attention was given to the hue component, as it directly measures color variation, independent of lighting conditions.

Similarly, the YCbCr color space commonly used in video compression and image processing, YCbCr separates luminance (Y) from chrominance (Cb and Cr) [23, 24]. This makes it more ideal for detecting color changes while minimizing or ignoring impact of changes in light intensity. The YCbCr space was used to highlight the chromatic differences between unripe and ripe paddy, which focusing on the shift from greenish hues to yellowish tones.

Additionally, the L*a*b* color space is a perceptually uniform color space that mimics human color perception by separating lightness L* from chromatic components which a* for the red-green axis and b* for the blue-yellow axis [21, 25]. It is chosen due to able to represent color differences as perceived by human vision accurately

Results and Discussion

Before proceeding to the image analysis, several image preprocessing methods were required to ensure the accuracy and consistency of the image data. These steps included image calibration, cropping and resolution adjustment, all of which were important to minimizing noise and ensuring that only relevant sections of the paddy field were analyzed. Following these image preprocessing, the images were ready for analysis in the RGB, HSV, YCbCr, and L*a*b* color spaces. The images after preprocessing, which ready for subsequent analysis are shown in Figure 5.

Figure 5. Image of unripe and ripe paddy field after preprocessing

RGB Color Space Analysis

The RGB histograms for ripe paddy fields are shown in Figure 6. For Red Channel (R), the histogram graph shows a concentration of pixel values in the mid-to-high intensity range and peaking around the 50 to 200 range. This indicates a strong presence of red hues and correlating with the yellowish color of ripe paddy. For Green Channel (G), there is a relatively broad distribution of green pixel values, with a noticeable concentration around the mid-range which is around 50 to 150. This suggests that while green is still present, it is diminishing as the ripeness level of paddy increases. For Blue Channel (B), the blue values are concentrated in the lower intensity range, which is around 0 to 100, this showing a weak presence of blue in the image, which is expected as the ripe paddy shifts towards a yellow or golden hue.

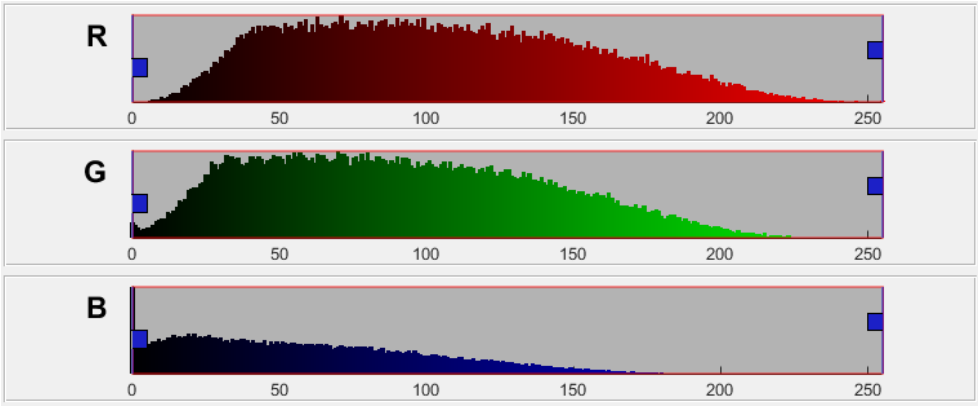

Figure 6. RGB color space analysis for ripe paddy

The RGB histograms for unripe paddy fields are shown in Figure 7. For the Red Channel (R), the histogram exhibits a wider distribution across the intensity spectrum, with a slight peak in the mid-range, indicating a balanced representation of red intensity levels in the image. This indicates a lesser dominance of red hues, as the unripe paddy is primarily green. For the Green Channel (G), it shows a more pronounced peak in the mid-to-high intensity range which is around 100 to 200 and highlighting the dominance of green hues in the unripe paddy. For Blue Channel (B), it exhibits lower intensity values, indicating minimal presence of blue in both stages which similar with the ripe paddy. However, the spread of blue values is slightly more evident in the unripe stage.

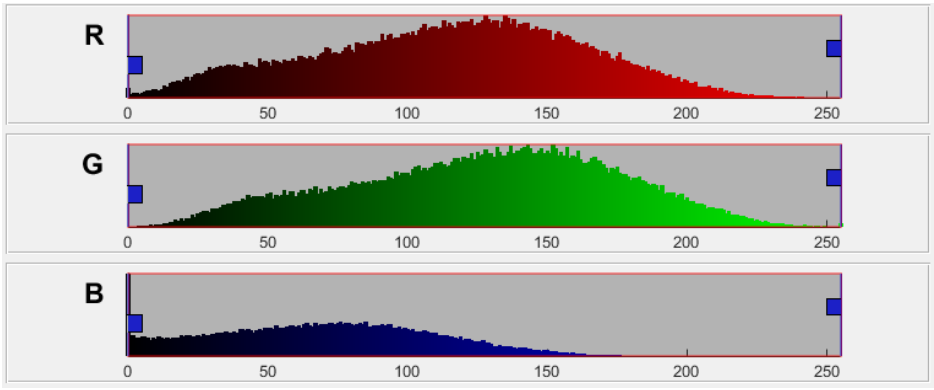

Figure 7. RGB color space analysis for unripe paddy

HSV Color Space Analysis

The HSV color space analysis for ripe paddy is shown in Figure 8 whereas HSV color space analysis for unripe paddy is shown in Figure 9. Firstly, the circular plot on the left-hand side corresponds to the Hue component, it shows a concentration of hues between approximately yellow to red for the ripe paddy. Hence, this finding shows that the ripe sample has a dominant red to yellow hue, which is also shown in mature stage.

In contrast, the unripe sample showed a much narrower range of hues, concentrated closer to the green spectrum. This indicates that unripe paddy predominantly reflect hues characteristic of immature stages of ripening, it is because green is commonly associated with early ripening stages in paddy.

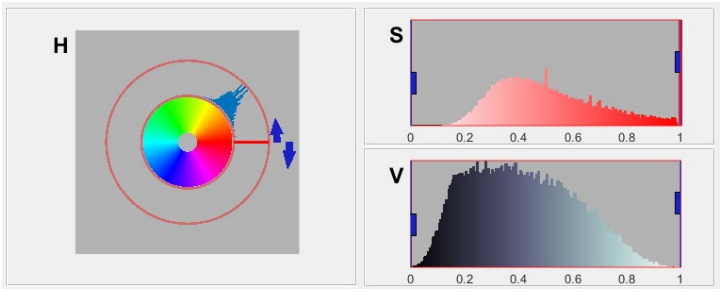

Figure 8. HSV color space analysis for ripe paddy

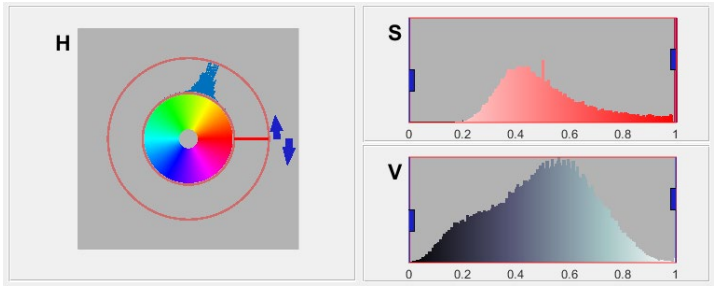

Figure 9. HSV color space analysis for unripe paddy

The saturation histograms show the difference in color intensity between the ripe and unripe paddy. The ripe paddy sample shows a lower saturation range, peaking around 0.4. This lower saturation indicates that the colors are less vivid, characteristic of the yellow hues of unripe paddy. On the other hand, the unripe paddy's saturation values are pointed toward the higher end, which ranging from 0.4 to 0.9, with an obvious peak around 0.4. This indicates that the unripe paddy has more vivid and intense green colors.

The value of brightness histograms has further distinguished the unripe paddy from the ripe paddy. The unripe paddy sample shows a higher concentration of brighter values which are between 0.4 and 0.6. This increased brightness may be attributed to the reflective surface of the immature paddy, which still retains moisture and is more vibrant. In contrast, the ripe paddy's value distribution is skewed towards lower brightness values, ranging between 0.2 and 0.6, reflecting the more matte and less reflective surface characteristic of ripe paddy.

YCbCr Color Space Analysis

The YCbCr color space histograms were used to analyses the color characteristics of ripe and unripe paddy. In this study, the Y component represents luminance or brightness, while Cb and Cr components represent the chrominance information or known as color differences as mentioned in previous section. The YCbCr color space analysis for ripe paddy is shown in Figure 10 whereas YCbCr color space analysis for unripe paddy is shown in Figure 11.

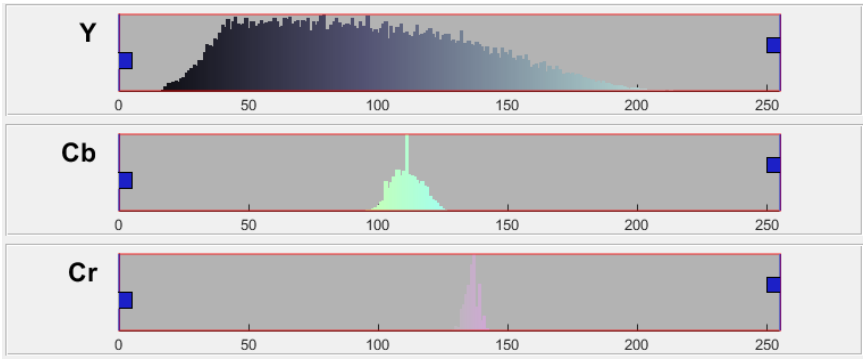

Figure 10. YCbCr color space analysis for ripe paddy

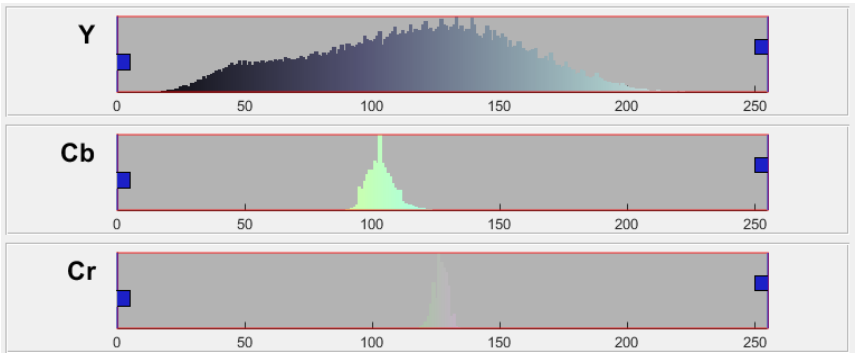

Figure 11. YCbCr color space analysis for unripe paddy

The Y luminance histogram of both ripe and unripe paddy shows a spread of values from 0 to 200, which indicates a range of brightness levels in both ripe and unripe paddy.

In addition, the Cb histogram of the ripe paddy shows a broader distribution and concentrated peak around 100 to 130 range. In contrast, the unripe paddy displays a concentrated peak around the 100 to 110 range with a relatively narrow distribution. The narrower distribution in the unripe paddy indicates a more uniform and specific blue chrominance, while the ripe paddy shows a wider range and shows a less consistent blue color tone.

Moreover, the Cr histogram peak for ripe paddy is around 140 and for unripe paddy is around 125, this result indicates a higher red chrominance in the ripe paddy. As the paddy ripens, it appears that the red component increases, contributing to a more reddish or warmer tone in its color wheres the unripe paddy has less red component in its color.

L*a*b* Color Space Analysis

The L*a*b* color space analysis was performed to distinguish between the unripe and ripe paddy samples. The histograms for the L*, a*, and b* channels as shown Figures 12 and 13, which represent the distribution of color values for the ripe and unripe paddy.

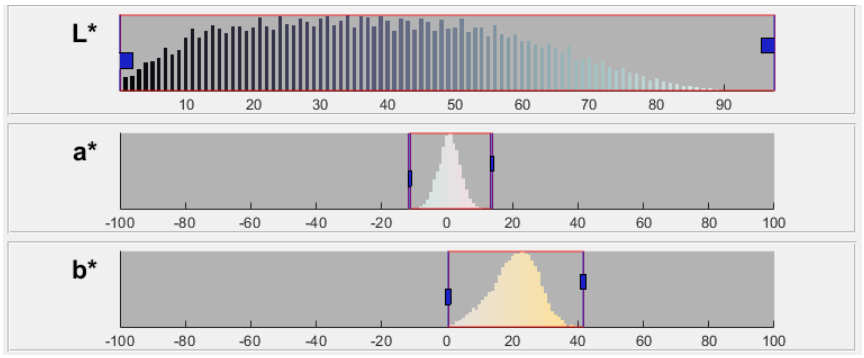

Figure 12. L*a*b* color space analysis for ripe paddy

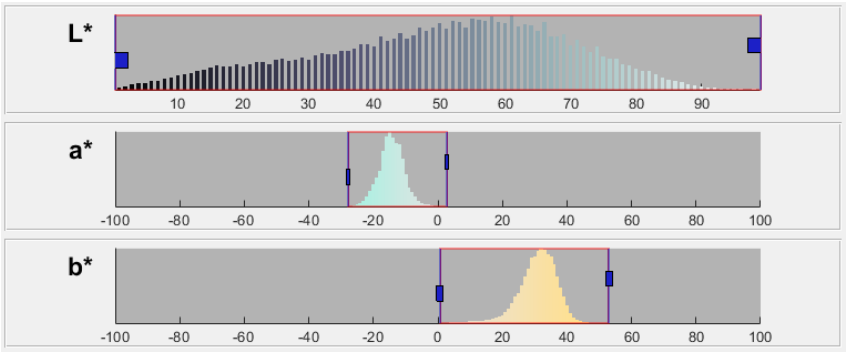

Figure 13. L*a*b* color space analysis for unripe paddy

In the ripe paddy, the L* values are predominantly concentrated between 10 and 50, with a gradual decline towards higher values, indicating a darker overall appearance characteristic of ripe paddy. Conversely, for the unripe paddy, the L* values are more broadly distributed, peaking between 40 and 70. This shift towards higher L* values correspond to a lighter appearance, which is typical of unripe paddy.

The ripe paddy shows a distribution of a* values approximately centred to 0 with a slight tendency towards positive values, which indicating a faint red hue. In contrast, the unripe paddy displays a clear shift towards negative a* values which peaking around -20, this reflects the greenish tint typically observed in unripe paddy. This difference in the a* channel can be known as a one of key indicator of the ripening process, where the green hue diminishes as the paddy ripens.

In addition, the ripe paddy's b* values are concentrated between 0 and 40, this suggesting a strong yellow hue, which is a characteristic of ripe paddy (yellow). However, the unripe paddy exhibits a wider distribution in the b* channel, which is ranging from approximately 20 to around 40 and with a peak around 30. While both unripe and ripe paddy display a yellow hue, the broader distribution in the unripe paddy sample set indicates a more varied color profile, which might cause from attributed to the transition stages within the unripe paddy sample set.

Discussion

For RGB color space analysis, the ripe paddy shows a shift towards higher red intensity values and lower green intensities compared to the unripe paddy, this result reflecting the transition from green to yellow as the paddy matures. Then, the blue channel remains relatively low in both stages and though with minor differences, this shows further emphasizing the color shift's reliance on the red and green channels for ripeness detection.

Moreover, the HSV analysis shows significant colorimetric differences between ripe and unripe paddy samples. Although the ripe paddy shows a wider range of hues in the yellow spectrum and lower saturation levels, whereas the unripe paddy shows brighter values, which reflecting a more vibrant and reflective surface. These findings provide a detailed quantitative assessment of the color changes that occur during paddy ripening and contribute to the understanding of how color spaces can be used to track crop maturity.

Moreover, the YCbCr color space analysis shows significant differences between ripe and unripe paddy samples in terms of luminance and chrominance. From the result, the ripe paddy increase in red chrominance (Cr) as the paddy ripens and a relatively lower red chrominance in the unripe paddy. This finding suggested that YCbCr color space characteristics, especially the chrominance differences and it can effectively distinguish between ripe and unripe paddy and potentially serving as an indicator for ripeness detection.

The L*a*b* color space analysis effectively differentiates between the unripe and ripe paddy samples. The ripe paddy is characterized by lower L* values, suggesting a darker appearance, approximately zero a* value which indicating the minimal presence of green, and a concentrated b* value which reflective of its characteristic yellow hue. In contrast, the unripe paddy shows higher L* values, indicating a lighter appearance, shift towards negative a* values which reflecting its greenish color and a broader b* distribution which indicating a varied yellow hue. These colorimetric differences align with the expected visual characteristics of paddy at different stages of ripeness, confirming the utility of the L*a*b* color space in ripeness assessment. The comparison between RGB, HSV, YCbCr and L*a*b* color space analysis of ripe and unripe paddy is shown in Table 1.

Table 1. Comparison for RGB, HSV, YCbCr and L*a*b* color space analysis of ripe and unripe paddy

Color Space	Channel	Ripe Paddy Characteristics	Unripe Paddy Characteristics	Estimated Difference (%)
RGB	Red (R)	Concentration in the mid-to-high range (50-200), strong red hues	Wider distribution across intensity spectrum, less dominant red hues	Moderate (~30% to 40%)
	Green (G)	Broad distribution, concentration around mid-range (50-150), diminishing green	Pronounced peak in mid-to-high range (100-200), dominant green hues	Strong (~50%)
	Blue (B)	Lower intensity and weak blue presence	Lower intensity and weak blue presence	Weak (~10% to 15%)
HSV	Hue (H)	Concentrated between red to yellow	Narrow range, concentrated closer to green spectrum	Strong (~50%)
	Saturation (S)	Lower saturation, peaking around 0.4, less vivid colors, characteristic of ripe yellow hue	Higher saturation, ranging from 0.4 to 0.9, more vivid and intense green hues	Moderate (~30% to 40%)
	Value (V)	Lower brightness (0.2-0.6), less reflective	Higher brightness (0.4-0.6), more reflective surface,	Weak (~10% to 20%)
YCbCr	Luminance (Y)	Spread of values from 0 to 200, range of brightness levels	Spread of values from 0 to 200, similar brightness levels	Weak (~5% to 10%)
	Blue Chrominance (Cb)	Broader distribution, concentrated peak around 100-130	Narrower distribution, concentrated peak around 100-110, more uniform blue chrominance	Moderate (~25% to 30%)
	Red Chrominance (Cr)	Peak around 140, higher red chrominance, warmer tone	Peak around 125, lesser red chrominance	Strong (~50%)

Color Space	Channel	Ripe Paddy Characteristics	Unripe Paddy Characteristics	Estimated Difference (%)
L*a*b*	Lightness (L*)	Concentrated between 10-50, darker appearance	Broadly distributed, peaking between 40-70, lighter appearance	Strong (~60%)
	Green-Red Axis (a*)	Centered around 0, slight tendency towards positive values (faint red)	Peaks around -20, strong green hue	Strong (~80%)
	Yellow-Blue Axis (b*)	Concentrated between 0-40, strong yellow hue	Broader distribution between 20 to 40, peak around 30	Strong (~70%)

The L*a*b* color space demonstrates the highest distinction between ripe and unripe paddy, with differences of 60-80% across its L* (lightness), a* (green-red), and b* (yellow-blue) channels. In contrast, YCbCr shows a moderate distinction, particularly in Cr (red chrominance) with around ~50% difference, but its Y (luminance) channel overlaps significantly between ripe and unripe paddy (5-10% difference). HSV provides better separation in Hue (H) and Saturation (S) (~50%), but its Value (V) channel overlaps (10-20% difference), which might reduce effectiveness. RGB performs the worst, with weak distinctions in the Red (R) (~30-40%) and Blue (B) (~10-20%) channels. From this study, the L*a*b* color space analysis is chosen as best option for color space analysis after comparing with RGB, HSV and YCbCr color space analysis. As L*a*b* color space provides a clear and quantifiable differentiation between ripe and unripe paddy, especially in the a* (green-red) and b* (yellow-blue) channels and colorimetric differences almost same with the expected visual characteristics of paddy at different stages of ripeness. Hence, L*a*b* color space analysis can be known as offers consistent and accurate data making it easier to assess the paddy maturity.

The demonstrated effectiveness of the L*a*b* color space enables machine learning models to utilize its features for automated paddy maturity classification. Traditional models such as Support Vector Machines (SVM) and K-nearest neighbors (KNN) can be employed for feature-based classification, which particularly leveraging the a* (green-red) and b* (yellow-blue) channels [26, 27]. In addition, deep learning models, particularly fully convolutional neural networks (FCNs), have been widely applied in remote sensing tasks for their ability to extract complex feature representations [28]. However, the use of high-resolution networks (HRNet) remains relatively underexplored. HRNet preserves high-resolution representations throughout the network, which ensuring enhanced spatial feature extraction for more precise classification. Furthermore, integrating reinforcement learning (RL) with deep learning-based paddy classification can facilitate the development of autonomous systems capable of real-time assessment and adaptive decision-making [29]. RL-based models can continuously learn and adjust to varying environmental conditions, thereby optimizing classification performance and enhancing harvesting strategies over time.

Conclusions

In this study, we conducted a comprehensive analysis of the color characteristics of ripe and unripe paddy using four different color spaces which are RGB, HSV, YCbCr, and L*a*b*. Each color space provided valuable insights into the paddy's ripeness stages. L*a*b* color space analysis is recommended as the preferred method for ripeness detection in paddy. In future, the color space analysis can be integrated with machine learning algorithms and will help to automate and enhance the accuracy of ripeness detection and allowing for real-time, large-scale assessments in agricultural practices. This new method of work can be led to the development of artificial intelligence system that able to be monitoring crop maturity, optimizing harvest timing and improving yield quality in paddy cultivation.

Conflicts of Interest

The authors declare that there is no conflict of interest regarding the publication of this paper.

Acknowledgement

This research was funded by the Ministry of Higher Education (MoHE) Malaysia with the Fundamental Research Grant Scheme (FRGS) under grant number FRGS/1/2021/TK0/UKM/02/17, and by the National Research and Innovation Agency (BRIN) Indonesia under the Perjanjian Pendanaan Program Riset dan Inovasi untuk Indonesia Maju Gelombang 4, with grant numbers 20/IV/KS/11/2023 and 1181/PL4.7.4.2/PT/2023.

References

[1] Firdaus, R. B. R., Leong Tan, M., Rahmat, S. R., & Senevi Gunaratne, M. (2020). Paddy, rice and food security in Malaysia: A review of climate change impacts. *Cogent Social Sciences, 6*(1), 1818373. https://doi.org/10.1080/23311886.2020.1818373

[2] Se, C. H., Khor, B. H., & Karupaiah, T. (2015). Prospects in development of quality rice for human nutrition. *Malaysian Applied Biology, 44*(2), 1–31.

[3] Dorairaj, D., & Govender, N. T. (2023). Rice and paddy industry in Malaysia: Governance and policies, research trends, technology adoption and resilience. In *Frontiers in Sustainable Food Systems* (Vol. 7). Frontiers Media S.A. https://doi.org/10.3389/fsufs.2023.1093605

[4] Ikhwali, M. F., *et al.* (2022). A review of climate change studies on paddy agriculture in Indonesia. *IOP Conference Series: Earth and Environmental Science, 1116*(1). https://doi.org/10.1088/1755-1315/1116/1/012052

[5] Kasim, N. B. M., *et al.* (2018). Food choices among Malaysian adults: Findings from Malaysian Adults Nutrition Survey (MANS) 2003 and MANS 2014. *Malaysian Journal of Nutrition, 24*(1).

[6] Omar, S. C., Shaharudin, A., & Tumin, S. A. (2019). *The status of the paddy and rice industry in Malaysia*. Khazanah Research Institute.

[7] Sari, R. K. (2014). Analisis impor beras di Indonesia. *Economics Development Analysis Journal, 3*(2).

[8] Firdaus, R. B. R., Ibrahim, A. Z., Siwar, C., & Jaafar, A. H. (2014). The livelihood of paddy farmers in facing challenges of climatic change: The role of government intervention through paddy price subsidy scheme. *Kajian Malaysia, 32*(2), 73–92.

[9] Tang, K. H. D. (2019). Climate change and paddy yield in Malaysia: A short communication. *Global Journal of Civil and Environmental Engineering, 1*, 14–19.

[10] Vaghefi, N., *et al.* (2016). Impact of climate change on food security in Malaysia: Economic and policy adjustments for rice industry. *Journal of Integrative Environmental Sciences, 13*(1), 19–35.

[11] Chou, Y. S., & Chou, C. Y. (2023). Deep learning approach for paddy field detection using labeled aerial images: The case of detecting and staging paddy fields in central and southern Taiwan. *Remote Sensing, 15*(14), 3575.

[12] Quamar, M. M., *et al.* (2023). Advancements and applications of drone-integrated geographic information system technology—A review. *Remote Sensing, 15*(20), 5039.

[13] Vigneault, P., *et al.* (2024). An integrated data-driven approach to monitor and estimate plant-scale growth using UAV. *ISPRS Open Journal of Photogrammetry and Remote Sensing, 11*, 100052. https://doi.org/10.1016/j.ophoto.2023.100052

[14] Slimani, H., El Mhamdi, J., & Jilbab, A. (2024). Assessing the advancement of artificial intelligence and drones' integration in agriculture through a bibliometric study. *International Journal of Electrical & Computer Engineering, 14*(1).

[15] Wang, R., Hu, F., & Wu, W. (2021). Estimation of paddy rice maturity using digital imaging. *International Journal of Food Properties, 24*(1), 1403–1415. https://doi.org/10.1080/10942912.2021.1970581

[16] Haw, C. L., *et al.* (2014). Colour vision to determine paddy maturity. *International Journal of Agricultural and Biological Engineering, 7*(5), 55–63. https://doi.org/10.3965/j.ijabe.20140705.006

[17] Hugar, S. M., & Abdul Waheed, M. (2021). Paddy yield estimation by identifying disease affected region. *2021 IEEE International Conference on Mobile Networks and Wireless Communications (ICMNWC)*, 1–7. https://doi.org/10.1109/ICMNWC52512.2021.9688526

[18] Abubakar, S., *et al.* (2022). Comparison of RGB and white LED illumination in honey imaging system using histogram approach. In *2022 IEEE 20th Student Conference on Research and Development (SCOReD)* (pp. 134–139). IEEE.

[19] Kumar, T., & Verma, K. (2010). A theory based on conversion of RGB image to gray image. *International Journal of Computer Applications, 7*(2), 7–10.

[20] Hassan, F. S., & Gutub, A. (2022). Improving data hiding within colour images using hue component of HSV colour space. *CAAI Transactions on Intelligence Technology, 7*(1), 56–68.

[21] Bora, D. J., Gupta, A. K., & Khan, F. A. (2015). Comparing the performance of L*A*B* and HSV color spaces with respect to color image segmentation. *arXiv preprint arXiv:1506.01472*.

[22] Sural, S., Qian, G., & Pramanik, S. (2002). Segmentation and histogram generation using the HSV color space for image retrieval. In *Proceedings. International Conference on Image Processing* (Vol. 2, pp. II–II). IEEE.

[23] Gopinathan, S., & Gayathri, M. S. (2016). A study on image enhancement techniques using YCbCr color space methods. *International Journal of Advanced Engineering Research and Science, 3*(8), 236818.

[24] Al-Ani, M., & Hammouri, T. A. (2011). Video compression algorithm based on frame difference approaches. *International Journal on Soft Computing, 2*(4), 67.

[25] Markovic, I., *et al.* (2013). Color measurement of food products using CIE L* a* b* and RGB color space.

[26] Raj, T., *et al.* (2021). Classification of oil palm fresh fruit maturity based on carotene content from Raman

spectra. *Scientific Reports, 11*(1), 18315.
[27] Malla, M. A., *et al.* (2024). Adopting machine learning to automatically identify a suitable surgery type for refractive error patients. *Jurnal Kejuruteraan, 36*(4), 1749–1757.
[28] Lim, S. V., *et al.* (2023). Attention-based semantic segmentation networks for forest applications. *Forests, 14*(12), 2437.
[29] Tan, J. L., *et al.* (2025). A review of reinforcement learning evolution: Taxonomy, challenges and emerging solutions. *International Journal of Advanced Computer Science & Applications, 16*(1).